ACS OMEGA

http://pubs.acs.org/journal/acsodf

Article

Unique Nonenzymatic Glucose Sensor Using a Hollow-Shelled Triple Oxide Mn−Cu−Al Nanocomposite

Nivedhini Iswarya Chandrasekaran and Manickam Matheswaran*

Cite This: *ACS Omega* 2020, 5, 23502−23509

Read Online

ACCESS | Metrics & More | Article Recommendations | Supporting Information

ABSTRACT: Glucose monitoring devices for diabetes mellitus, which is a worldwide significant health issue, have attracted attention of many researchers. Herein, we report a hollow Mn−Cu−Al oxide nanocomposite (HMCA) by a microwave-assisted technique showing excellent sensing abilities toward glucose. Also, it possesses a superb supercapacitor activity described in our previous paper. The sensitivity value of the nanocomposite is 2.194 mA mM^{-1} cm^{-2} with a low detection limit of 0.43 μM (S/N = 3). The high sensitivity and low detection limit were the results of the large surface area of the nanocomposite and the redox nature of CuO and MnO_2. It shows a selective detection of glucose levels in blood serum. The hollow nanocomposite has been useful for monitoring the glucose level in blood serum and holds great potential for diabetes mellitus and clinical diagnosis.

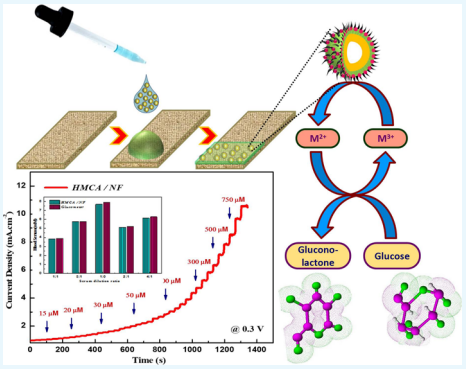

1. INTRODUCTION

Determination of glucose plays a very vital role in various fields such as clinical analysis, food technology, pharmaceutical chemistry, industrial and environmental applications, and so on[1] because active monitoring of glucose does many essential things in the field of biotechnology, clinical diagnosis, and in some food monitoring fields.[2] Previously, a glucose sensor has been developed based on glucose oxidase, which has high sensitivity.[3,4] Several disadvantages are found in the glucose oxidase based biosensor such as more profoundness to the thermal and chemical environment, stability issue, complexity, and poor reproducibility.[5−7] To overcome these issues, many efforts have been taken to identify glucose concentration without the help of enzymes. Pt, Au, Cu, and their alloys have employed for direct electro-oxidation of glucose.[8] Similarly, the electrodes modified with Ni, Cu, Ag, Hg, and Bi have been explored as capable enzymeless sensors. However, these mentioned electrodes have disadvantages of reduced sensitivity, low selectivity, and prone to chloride poisoning. Hence, it is appropriate to discover and develop a nonenzymatic glucose sensor with high sensitivity, fast response time, and excellent stability by electrochemical oxidation.

The nonenzymatic electrodes developed from bimetals, metal oxide nanoparticles, metallic composites, and metal alloys hold exceptional structural, chemical, and physical properties to improve the high sensitivity, fast response, and wide range of detection with a low detection limit of the sensor.[9] The bimetallic material could become a more significant catalyst that reveals preferred electronic property and catalytic activity. Alloys and metal oxide composites are the foremost systems of bimetallic electrocatalysts. Owing to the synergistic consequence of the two materials, the bimetallic materials can expressively improve the glucose oxidation and diminish the interference and poisoning effect of the sensing electrode. A binder-free Au/CuO nanocauliflower electrode possesses an excellent electrocatalytic activity and high sensitivity toward glucose oxidation.[10] Porous CuO−CdO composite nanofibers show good anti-interference, low detection limit, and fast response of glucose at 0.4 V, ascribing to the enhanced conductivity due to CdO, good electrocatalytic activity due to CuO, and large surface area owing to porous structure.[11] The synergistic effect between NiO@Fe_3O_4-SH directed to notable improvements such as linear dynamic range, low detection limit, and acceptable potential in the detection of glucose.[12]

Comparatively, the analytic devices built using transition metal oxide are cheap and more sensitive because of surface area and selectivity nature.[13] Predominantly, metal oxides, such as ZnO,[14] Cu_2O,[15,16] MnO_2,[17] TiO_2,[18] SnO_2,[19] Co_3O_4,[20] NiO,[21] and so forth, have been reported as sensitive electrode materials for the determination of glucose. Among all CuO is an eco-friendly p-type semiconductor material that has a narrow band gap of 1.2 eV. It has been widely used in various fields such as optical, electrical, photovoltaic system, catalysis, sensor, magnetic storage media, and so forth.[16,22] Excellency in

Received: January 30, 2020
Accepted: April 14, 2020
Published: September 12, 2020

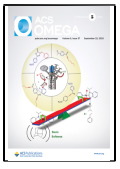

https://dx.doi.org/10.1021/acsomega.0c00417
ACS Omega 2020, 5, 23502−23509

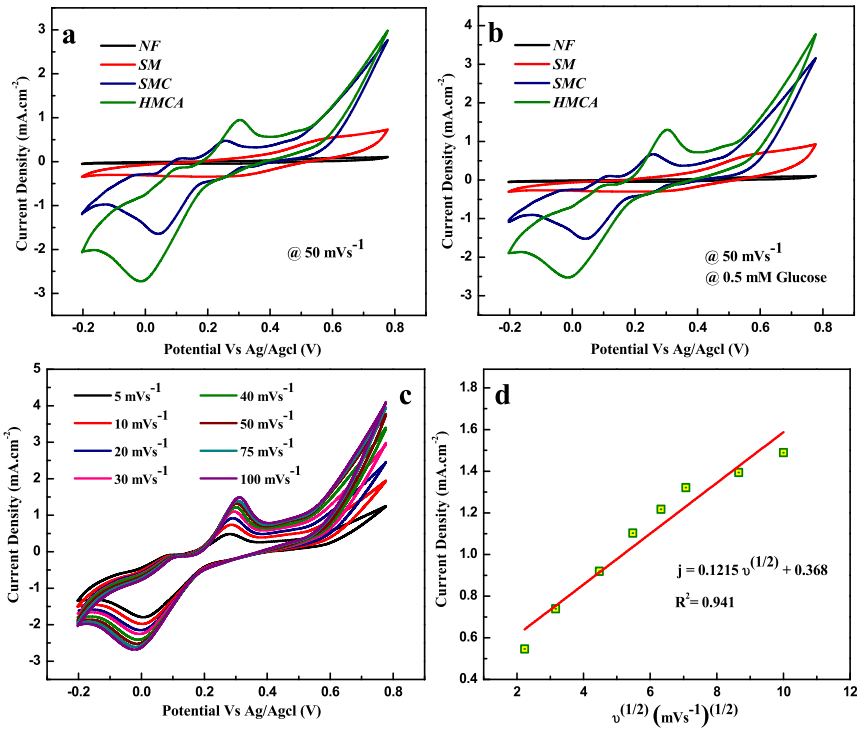

Figure 1. Cyclic voltammograms of as-prepared nanocomposite-modified electrodes in the absence (a) and presence (b) of 0.5 mM glucose in 0.1 M NaOH at a scan rate of 50 mV s^{-1}. (c) Cyclic voltammograms acquired by HMCA/NF in 0.1 M NaOH in the presence of 0.5 mM glucose. The scan rate ranges from 5 to 100 mV s^{-1}. (d) Plot of peak current vs square root of scan rate.

multiple areas is owing to the virtue of low cost, exceptional catalytic activities, free of hazards, good electrochemical behavior, and eco-friendly nature. Particularly in the field of sensors, it shows excellent behavior such as good electrochemical stability, vibrant activity, high specific surface area, suitable redox properties, and superior chemical and thermal stability.[23,24] Also, manganese dioxide has possessed many advantages economically and environmentally. Also, it has drawn significant research interest owing to its intrinsic redox nature and best electrocatalytic activities toward carbohydrates, hydrogen peroxide, and oxygen reduction.[25,26] The literature says the former one (CuO) exhibits high selectivity and a wide range of detection limits, while the latter one (MnO_2) supports for low detection limit and fast response.

It is familiar that the dimension and shape of nanomaterials play a significant role in the electrochemical sensor compared with the bulk material.[27,28] Compositing of metal oxide in the desired shape and size improves the electrochemical performance and stability.[29,30] The excellent compatibility and superior catalytic property of MnO_2 have been utilized with CuO to design a hollow triple oxide material as a nonenzymatic sensing material for glucose determination. The presence of Al_2O_3 improves the electrical conductivity of the composites. The as-prepared hollow nanocomposite electrode has exceptional electrocatalytic activities and is also made up of a lasting electrode for observing blood glucose levels in samples at low manufacturing cost. The enhanced sensitivity with high selectivity toward glucose is mainly because of the abundant availability of active sites, practical usage of active material, fast mass transport, and high electrical conductivity nature of nanocomposites.

2. RESULTS AND DISCUSSION

2.1. Formation Mechanism and Physiochemical Properties. The modified Stober method is employed for the preparation of core SiO_2. The controlled morphology is obtained by using a stabilizing agent, CTAB. The introduction of Mn^{2+} precursor results in the formation of a shell layer by developing a coordination compound with a hydroxyl group from urea. An electrostatic interaction between oxides and metal cations fixes the Cu^{2+} ions over the surface of SiO_2@ MnO_2, which results in the formation of the CuO layer. Further addition of Al^{3+} ions from $Al(NO_3)_3$ results in the formation of Al_2O_3. Last, hollow structures have been achieved with triple oxide materials.[31] In this formation procedure, successive treatment with urea provides an alkaline environment, which favors for dissolution of core SiO_2 that results in a hollow structure. This SiO_2 will neutralize in the essential medium by forming silicates as a result of breaking the Si−O−Si bond. The hydrolysis of urea results in an alkaline solution by forming ammonia and carbon dioxide.[32]

$$CO(NH_2)_2 + 3H_2O \rightarrow CO_2 + 2NH_4^+ + 2OH^-$$

Etching of silica core took place simultaneously by OH^- released from the hydrolysis of urea. Here, urea not only served as a reducing agent for the formation of metal oxide but also provide a hollow nanostructure by delivering a mildly alkaline environment to remove SiO_2 gradually. As a result of successive treatment, a delicate hollow nanocomposite structure formed from MnO_2, CuO, and Al_2O_3 (HMCA).

The specific surface area obtained from N_2 adsorption and desorption was about 24.12, 94.29, 201.84, and 310.36 m^2 g^{-1} for S, SM, SMC, and HMCA, respectively. Figure S1 (Supporting Information) provides the N_2 sorption isotherms and the respective pore size distribution of all samples. Results

https://dx.doi.org/10.1021/acsomega.0c00417
ACS Omega 2020, 5, 23502−23509

clearly define that HMCA possesses a type IV adsorption isothermal curve with an H4-type hysteresis loop, which generally proves the narrow slit-like pores with mesoporous size and internal voids of irregular shape. The outcomes show that HMCA possesses a higher surface area, and this increased surface area is believed to increase the catalytic activity of the nanocomposites.

Figure S2a−d (Supporting Information) provides the morphological structure of nonagglomerated and monodispersed S, SM, SMC, and HMCA, respectively. Successive coating provides the hairy appearance to the HMCA nanocomposites. Also, the image clearly gives the idea about the disappearance of the core structure on subsequent coating. As a result, a hollow structure is attained during HMCA formation. This distinct morphology supports for glucose fixation effectively. Figure S2g shows the HRTEM image of HMCA, which clearly distinguishes the high crystalline region (shell) and low crystalline region (hairy morphology) with a clear interface. The calculated lattice distance from Figure S2h matches well with the (1 1 0) plane of Al_2O_3. Figure S2i shows that the SAED pattern of the HMCA nanocomposite material is paired with the JCPDF card: 01-1117. Multielemental EDS mapping of an HMCA is shown in Figure S2j, which is consistent with the EDS spectrum shown in Figure S2f, as well as the surface roughness nature of HMCA supporting Brunauer−Emmett−Teller surface area results.

Figure S3 (Supporting Information) provides the X-ray photoelectron spectroscopy (XPS) spectrum for HMCA nanocomposites. The XPS wide spectrum (Figure S3a) shows the presence of Cu, Mn, O, and Al in the prepared nanocomposites. The inset of Figure S3a shows the peak position of O 1s state at 534.36 eV. Figure S3b−d shows the individual high-resolution spectra of Mn 2p, Cu 2p, and Al 2p, respectively. The individual XPS spectrum of Mn 2p exhibits two prominent peaks at 645.16 and 656.08 eV with 11.2 eV of spin energy separation corresponding to the Mn $2p_{3/2}$ and Mn $2p_{1/2}$ spin−orbit peaks of MnO_2. Moreover, the atom molar rate of O is higher when compared to Mn in the survey spectrum, demonstrate the formation of MnO_2, and its chemical state is 4+. The result was compared with the early reported MnO_2 data. The higher oxidation state of manganese species has more active sites for electrocatalytic features. The remarkable peaks in the high-resolution spectrum of Cu 2p (Figure S3c) around 934.7 and 952 eV correspond to Cu $2p_{3/2}$ and Cu $2p_{1/2}$ of CuO. These results specify the copper exit in the valence state of 2+. The presence of Cu^{2+} affirmed the good charge-transfer nature, which results from excellent interaction between both oxides (catalyst-free fabrication of novel ZnO/CuO core−shell nanowire heterojunction: controlled growth and structural and optoelectronic properties). The spectrum of Al 2p shows the peak at 71.1 and 76.9 eV owing to the presence of Al_2O_3 shown in Figure S3d. The elemental composition and oxidation state of metallic cations have been clearly supporting the oxide formation.[31]

2.2. Electrocatalyst of Glucose on Nanocomposite-Modified Ni Foam. The catalytic activity of nanocomposite electrodes on glucose oxidation in 0.1 M of NaOH solution is proved by cyclic voltammetry (CV) in Figure 1. The plot explains the CV of 0.5 mM glucose in a NaOH solution at a scan rate of 50 mV s^{-1}. The presence (Figure 1b) and absence (Figure 1a) of glucose do not show any response on Ni foam. A pair of quasi-reversible redox peaks is observed in SM, which can be assigned to a Mn^{2+}/Mn^{3+} redox couple, while the Ni foam does not show any peak. However, a multiple redox peak is observed in SMC and HMCA, which corresponds to both Mn^{2+}/Mn^{3+} and Cu^{2+}/Cu^{+} redox couples. There is no change in the peak position on the addition of Al_2O_3 in HMCA while comparing it with SMC, which proves the inert electrochemical activity of Al_2O_3. Also, HMCA displays higher current value than those obtained from SMC, which attribute to improved stability and enhanced conductivity because of the presence of Al_2O_3.[33] Upon glucose addition, the oxidative peak current obtained at SM, SMC, and HMCA electrodes is increased, which can be attributed to the catalytic effect of the redox couple for the oxidation of glucose to gluconolactone shown in Figure 1b.

$$MnOOH + C_6H_{12}O_6(glucose) \rightarrow MnO_2 + C_6H_{10}O_6(gluconolactone)$$

$$CuOOH + C_6H_{12}O_6(glucose) \rightarrow CuO + C_6H_{10}O_6(gluconolactone)$$

The response belonging to irreversible glucose oxidation is observed at each electrode. Compared with other electrodes, HMCA shows a negative shift in peak potential. This proved the high electrocatalytic activity of HMCA on direct oxidation of glucose. The shifted potential was attributed to the effect of increased electroactive surface area and electron-transfer rate between glucose and HMCA electrode.[34] Moreover, the continuous increase in peak current until the potential of 0.6 V proved the involvement of redox species in glucose oxidation.[35] Further, CV of the HMCA electrode in the presence of glucose solution (0.5 mM) on different scan rates was performed as shown in Figure 1c. The peak current of glucose oxidation in the HMCA electrode is proportional to the scan rate and shows good linearity in the range of 5-100 mV s^{-1}, as shown in Figure 1d. It matches with the linear regression equation j (mA cm^{-2}) = $0.122\nu^{1/2}$ (mV s^{-1})$^{1/2}$ + 0.368 with a correlation coefficient of 0.941. The outcome shows that the electrochemical activity is controlled by glucose adsorption on the electroactive surface.

2.3. Mechanism of Glucose Oxidation. The reaction of MnO_2 in alkaline solution results in the formation of a hydroxide compound; as a result, Mn(III) oxyhydroxide is formed further on electro-oxidation. Immediately, glucose will be oxidized by producing a radical intermediate that responds rapidly with hydroxyl anions to create gluconolactone.

$$MnO_2 + 2OH^- \rightarrow MnOOH + H_2O + e^-$$

$$MnOOH + C_6H_{12}O_6(glucose) \rightarrow MnO_2 + C_6H_{10}O_6(gluconolactone)$$

Similarly, the catalytic reaction of CuO towards electro-oxidation of glucose depends on the redox couple of CuO/CuOOH

$$CuOOH + C_6H_{12}O_6(glucose) \rightarrow CuO + C_6H_{10}O_6(gluconolactone)$$

The overall mechanism of HMCA in glucose oxidation is

https://dx.doi.org/10.1021/acsomega.0c00417
ACS Omega 2020, 5, 23502−23509

$$MnOOH@CuOOH@Al_2O_3 + C_6H_{12}O_6(glucose) \rightarrow hollow\ MnO_2@CuO@Al_2O_3(HMCA) + C_6H_{10}O_6(gluconolactone)$$

2.4. Amperometric Response of Nanocomposite-Modified Ni Foam to Glucose. Figure 2 shows the chronoamperometric response of glucose oxidation in the HMCA electrode at various potentials on successive addition of 0.5 mM glucose in 0.1 M NaOH for every 30 s. Comparing the current responses on the HMCA electrode of glucose oxidation, the applied potential of 0.3 V provides higher response sensitivity and lower noise. Hence, 0.3 V was fixed as the optimum potential for chronoamperometric detection of glucose in further studies.

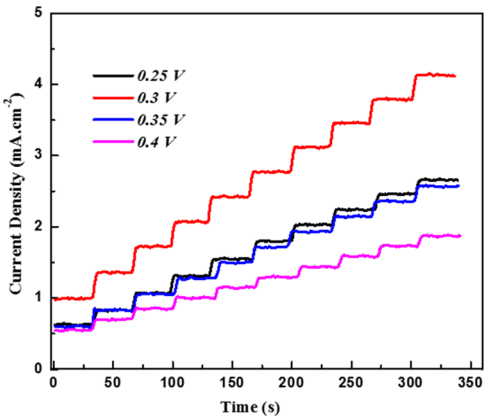

Figure 2. Amperometric response of HMCA/NF sensing electrode recorded at various applied potentials with the constant addition of 0.5 mM of glucose in 0.1 M NaOH.

The amperometric response of the HMCA electrode at 0.3 V with successive addition of glucose at various concentrations (5 μM to 1 mM) to 0.1 M NaOH solution under constant stirring is shown in Figure 3a. It was notable that the HMCA electrode displays a fast response to the addition of glucose by achieving its steady state current within 4 s. Figure 3b provides a sensitive current response to various glucose concentrations. The corresponding calibration curve shows the regression equation j (mAcm^{-2}) = 2.196c (mM) + 0.984 with a correlation factor of 0.991. The HMCA electrode exhibits exceptional linearity between the peak current and glucose concentration in the range of 5 μM to 2.5 mM, with a good sensitivity of 2.196 mA mM^{-1} cm^{-2} and a low detection limit of 0.43 μM at S/N of 3. Table 1 portrays the sensing comparison of our proposed material with other literature works. The presence of redox species significantly increases the electroactive sites and promotes electron transfer in the glucose oxidation process. Also, the porous morphology supports for fast diffusion of electrolytes into the electrode materials. Our HMCA sensor displays a satisfactory performance with features of higher sensitivity, rapid response time, and lower detection limit.

2.5. Reproducibility, Stability, and Selectivity Property of HMCA Electrode. The reproducibility nature of the HMCA electrode was evaluated by comparing the amperometric responses at 0.3 V for freshly prepared five different electrodes (Figure 4a,b). 2.57% of the relative standard deviation (RSD) value is confirming the high reproducible results of HMCA electrodes. Also, the successive measurement of glucose (0.5 mM) using various HMCA electrodes with an average RSD of 3.15% reveals the excellent reproducing nature of the HMCA electrode. The long-term stability of the HMCA electrode material was estimated by measuring the amperometric response regularly for once in 5 days (Figure 4c,d). The current response data reveal that the fabricated sensor keeps 79% of its initial response after 30 days, which proves the chemical stability and stable morphology of the HMCA nanocomposite.

Another valuable property is to investigate the selectivity nature of sensing electrode among other oxidative species such as dopamine, ascorbic acid, uric acid, and so on. These compounds usually exist in blood samples along with glucose and act as an interfering species in the electrochemical response of the electrodes. Figure 5 provides the amperometric response of the HMCA electrode by successive addition of glucose (0.5 mM) and interfering compounds (0.1 mM) in 0.1 M NaOH electrolyte solution. There is no significant change in amperometric response on the addition of interfering compounds that proves the highly selective nature of sensing electrode toward glucose detection. Additionally, the anti-poisoning quality of electrodes toward chloride ions has been tested by adding NaCl to the electrolyte solution because chloride ions will form a complexation with the metallic nanoparticle, which reduces the electrocatalytic nature of HMCA electrodes. In contrast, chloride ions are difficult to create a complex with metal oxide because the electronegativity of O is higher than Cl. The results show that the peak current

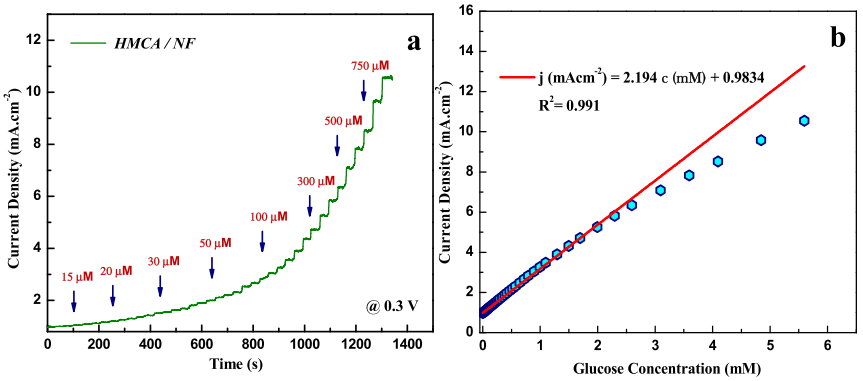

Figure 3. (a) Current−time response of the as-prepared HMCA/NF electrode at 0.3 V upon successive addition of different concentrations of glucose at an interval of 30 s. (b) Calibration curve of peak current vs concentration of glucose at the HMCA/NF electrode.

https://dx.doi.org/10.1021/acsomega.0c00417
ACS Omega 2020, 5, 23502−23509

Table 1. Comparison of Analytical Performance of Fabricated HMCA/NF Sensing Electrode with Other Proposed Nonenzymatic Sensors

sensing materials	detection potential (V)	sensitivity (μA mM^{-1} cm^{-2})	LOD (μM)	linear range	response time (s)	references
3D electrospun CuO nanofibers/GCE	0.4	431.3	0.8	6 μM to 2.5 mM	~1	36
ZnO−CuO HNCs/FTO glass plate	0.7	3066.4	0.21	0.47 μM to 1.6 mM	~2	37
β-MnO_2 micro/nanorod arrays/flexible carbon fiber fabric	0.55	1650.6	1.9	0.01 mM to 4.5 mM	<3	38
CuO nanoparticles/CNT	0.4	2596	0.2	0.4 μM to 1.2 mM	<1	39
Ni/MnO_2 nanocomposite/GCE	0.45	1040	0.1	0.25 μM to 3.5 mM	<3	40
CuO nanoparticles decorated carbon spheres	0.55	2981	0.1	0.5 μM to 2.3 mM	<5	41
Nafion/CuO nanoseeds/Au	0.6	1101	50	0.1 mM to 13.3 mM	~2	42
3D porous CNT/MnO_2 composite	0.6	3406.4	0.5	5 μM to 1 mM	<3	43
ZnO@N_2-doped carbon sheets (NDC)	0.75	231.7	6.3	0.2−12 mM	<3	44
HMCA/NF	0.3	2194	0.43	5 μM to 2.5 mM	<4	**present work**

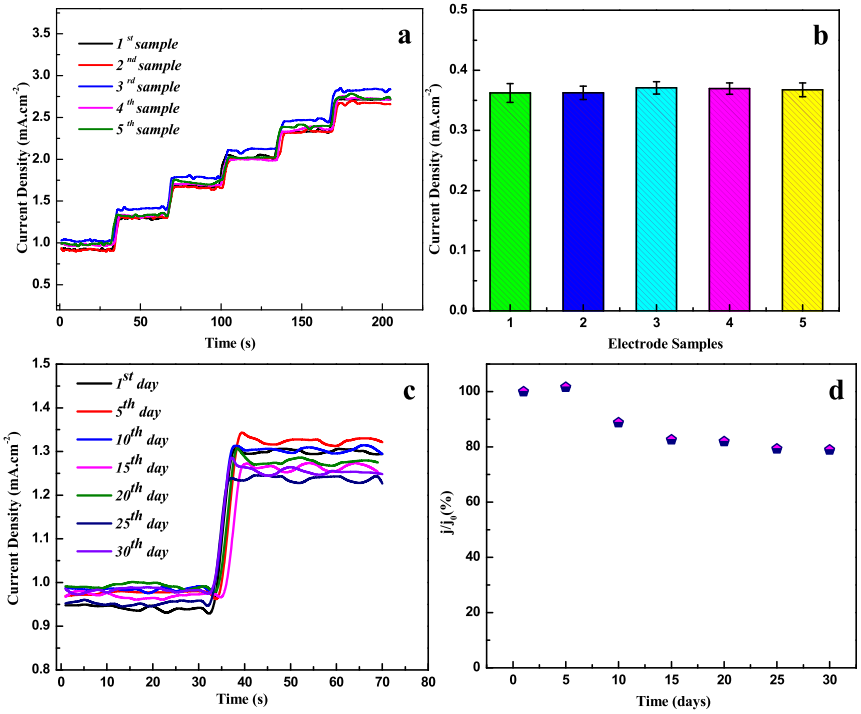

Figure 4. (a) Amperometric test results of five different HMCA/NF sensing electrodes conducted with the successive addition of 0.5 mM of glucose at 0.3 V. (b) Histogram with error bar shows repeatability results of different HMCA/NF electrodes. The error bar represents the standard deviation of the current response on the addition of 0.5 mM glucose. (c) Amperometric response of HMCA/NF electrode measured at room temperature for 1 month period at an interval of 5 days. (d) Long-term stability of HMCA/NF sensing electrode at room temperature.

of the HMCA electrode is almost the same on the addition of NaCl to the glucose-containing an electrolyte, indicating the antipoisoning nature of the electrode material.

2.6. Human Serum Sample Measurement. To analyze the performance of the HMCA electrode for real-time analysis, the electrode was engaged to find the glucose concentration in human serum samples by performing amperometric measurements (Figure 6a,b). Various concentrations of serum sample were added to 0.1 M NaOH solution, and the current response was recorded at 0.3 V. The response of human serum samples is slightly less than the response of commercial grade glucose and proves the presence of different biomolecules in serum samples, which limit the analytes diffuse into HMCA electrodes. The recovery test was performed to validate the HMCA sensor by comparing the obtained data with analytically measured values using a glucose monitoring kit (MAX Glucocard). Corresponding results are given in Table 2. For comparison, the obtained results and the results of the glucose monitoring kit (MAX Glucocard) are shown in the histogram chart (Figure 6c,d). These results confirm the potential of the HMCA electrode in the determination of glucose in human blood serum.

https://dx.doi.org/10.1021/acsomega.0c00417
ACS Omega 2020, 5, 23502−23509

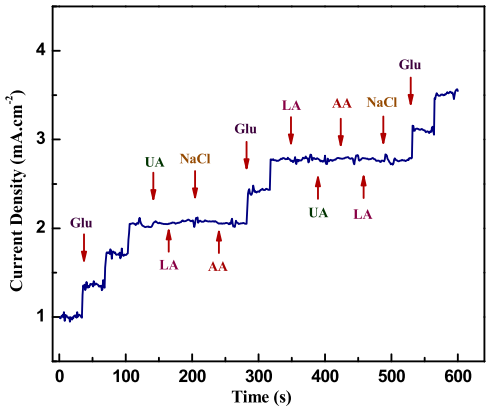

Figure 5. Current−time response of HMCA/NF on successive addition of 0.5 mM glucose and 1 mM interfering compounds (ascorbic acid, uric acid, and NaCl) in 0.1 M NaOH upon continuous stirring at 0.3 V.

3. CONCLUSIONS

The nonenzymatic glucose sensor is successfully fabricated using HMCA nanocomposites. The presence of a hollow structure with the porous morphology results in excellent electrocatalytic activity toward glucose oxidation in the HMCA/NF-modified electrode. The HMCA sensor electrode possesses excellent properties such as high sensitivity (2196 μA·mM^{-1} cm^{-2}), low detection limit (0.43 μM), wide linear range (5 μM to 2.5 mM), good reproducibility, sturdy stability, and excellent selectivity toward glucose determination. Additionally, the HMCA sensor was successfully applied in human blood serum to determine the glucose concentration. The composite holds the potential for effective nonenzymatic glucose determination with high sensitivity and low detection limit.

Table 2. Amperometric Determination of Glucose in Human Serum Samples

	sample 1		sample 2	
serum concentration (serum/DD)	HMCA/NF	glucometer	HMCA/NF	glucometer
1:1	3.10	3.08	3.84	3.89
3:1	4.65	4.72	5.76	5.74
1:0	6.20	6.18	7.68	7.86
2:1	4.13	4.07	5.12	5.23
4:1	4.96	5.03	6.14	6.28
error percentage	0.99		1.503	

4. EXPERIMENTAL SECTION

4.1. Synthesis and Fabrication of Nanocomposite Based on Glucose Sensing Electrode. A hollow-shelled triple oxide Mn−Cu−Al nanocomposite (HMCA) was prepared by microwave-assisted methods described elaborately in the previous work.[31] Briefly, 0.5 g of SiO_2, 0.05 M $MnSO_4$, and 0.015 M CH_4N_2O were prepared and treated in the microwave at 120 °C for about 1 h. The obtained powder was calcined in air at 200 °C for 2 h to get SiO_2@MnO_2 (SM). Further SiO_2@MnO_2@CuO (SMC) was prepared by calcining the microwave-treated product containing 0.5 g of SM, 0.05 M $Cu(NO_3)_2$, and 0.015 M CH_4N_2O. Finally, HMCA obtained the same by treating 0.5 g of SMC and 0.01 M of $Al(NO_3)_2$ with urea in microwave, followed by calcination. Nickel foam of 25 mm^2 was successively treated with HCl and ethanol, after which it was coated with nanocomposite suspension containing the dispersed nanocomposite in 1:5 ratio of Nafion

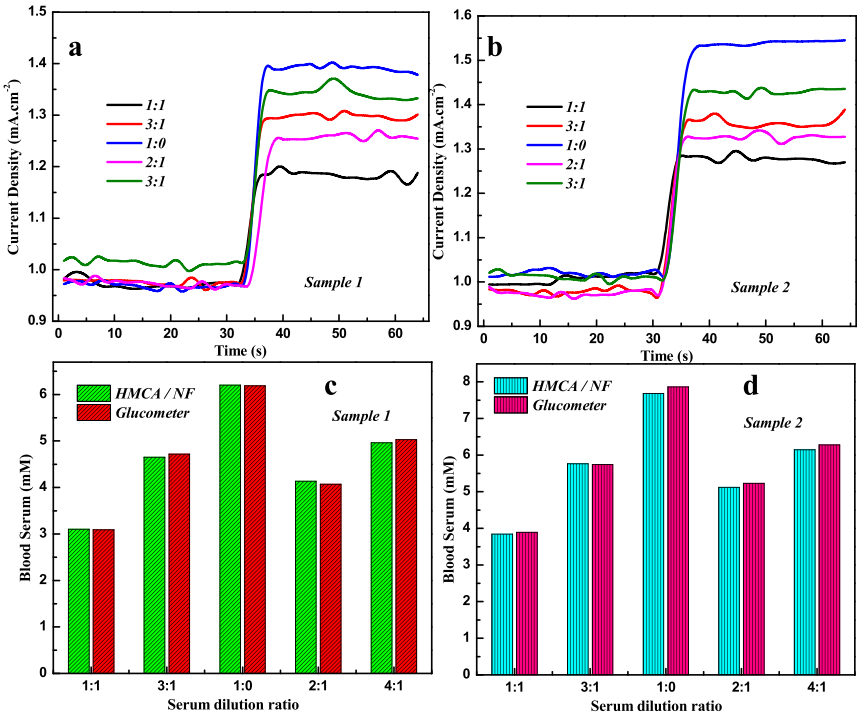

Figure 6. Current−time response of HMCA/NF sensing electrode in 0.1 M NaOH at 0.3 V on the addition of human blood serum sample 1 (a) and sample 2 (b). Histogram shows the determination of glucose concentration of human serum sample using HMCA/NF sensing electrode and glucometer for sample 1 (c) and sample 2 (d).

https://dx.doi.org/10.1021/acsomega.0c00417
ACS Omega 2020, 5, 23502−23509

and isopropanol solution mixed in a proportion of (1:5) to form the nanocomposite suspension. The coated foam is dried in a hot air oven for 60 °C to get modified nickel foam (SM/NF, SMC/NF, and HMCA/NF).

4.2. Electrochemical Measurements. The electrochemical measurement was performed in a three-electrode cell system using a PARSAT MC electrochemical workstation, in which the nanocomposite-supported Ni foam was employed as a working electrode, Ag/AgCl as a reference electrode, and platinum as a counter electrode. A solution of 0.1 M NaOH was used to perform CV and chronoamperometric procedure under a uniform stirring condition at room temperature. Glucose aliquots were added at a time interval of 30 s to achieve a steady current state in glucose sensing test. Before conducting the electrochemical measurement, the nanocomposite-modified electrode was dipped in the electrolyte for about 10 min.

■ ASSOCIATED CONTENT

Supporting Information

The Supporting Information is available free of charge at https://pubs.acs.org/doi/10.1021/acsomega.0c00417.

Physiochemical characterization of nanocomposites: graphics of N_2 adsorption−desorption isotherm with pore size distribution plot, TEM images, and XPS images of nanocomposites (PDF)

■ AUTHOR INFORMATION

Corresponding Author

Manickam Matheswaran − *Department of Chemical Engineering, National Institute of Technology Tiruchirappalli, Tiruchirappalli 620015, India;* orcid.org/0000-0002-5433-2188; Phone: +91-431-2503120; Email: math.chem95@gmail.com, matheswaran@nitt.edu; Fax: + 91-431-2500133

Author

Nivedhini Iswarya Chandrasekaran − *Department of Chemical Engineering, Indian Institute of Technology Madras, Chennai 600036, India;* orcid.org/0000-0003-4158-1705

Complete contact information is available at: https://pubs.acs.org/10.1021/acsomega.0c00417

Notes

The authors declare no competing financial interest.

■ ACKNOWLEDGMENTS

The authors are grateful to NIT, Tiruchirappalli, and MHRD, India, for financial support.

■ REFERENCES

(1) Marvin, J. S.; Hellinga, H. W. Engineering Biosensors by Introducing Fluorescent Allosteric Signal Transducers: Construction of a Novel Glucose Sensor. *J. Am. Chem. Soc.* **1998**, *120*, 7−11.

(2) Zhuang, Z.; Su, X.; Yuan, H.; Sun, Q.; Xiao, D.; Choi, M. M. F. An Improved Sensitivity Non-Enzymatic Glucose Sensor Based on a CuO Nanowire Modified Cu Electrode. *Analyst* **2008**, *133*, 126−132.

(3) Shan, C.; Yang, H.; Song, J.; Han, D.; Ivaska, A.; Niu, L. Direct Electrochemistry of Glucose Oxidase and Biosensing for Glucose Based on Graphene. *Anal. Chem.* **2009**, *81*, 2378−2382.

(4) Wilson, R.; Turner, A. P. F. Glucose Oxidase: An Ideal Enzyme. *Biosens. Bioelectron.* **1992**, *7*, 165−185.

(5) Sharp, P. Interference in Glucose Oxidase-Peroxidase Blood Glucose Methods. *Clin. Chim. Acta* **1972**, *40*, 115−120.

(6) Liu, Y.; Teng, H.; Hou, H.; You, T. Nonenzymatic Glucose Sensor Based on Renewable Electrospun Ni Nanoparticle-Loaded Carbon Nanofiber Paste Electrode. *Biosens. Bioelectron.* **2009**, *24*, 3329−3334.

(7) Yazid, S. N. A. M.; Akmar, S. N.; Md Isa, I.; Abu Bakar, S.; Hashim, N.; Ab Ghani, S. A Review of Glucose Biosensors Based on Graphene/Metal Oxide Nanomaterials. *Anal. Lett.* **2014**, *47*, 1821−1834.

(8) Basu, D.; Basu, S. Performance Studies of Pd−Pt and Pt−Pd−Au Catalyst for Electro-Oxidation of Glucose in Direct Glucose Fuel Cell. *Int. J. Hydrogen Energy* **2012**, *37*, 4678−4684.

(9) Xiao, F.; Zhao, F.; Mei, D.; Mo, Z.; Zeng, B. Nonenzymatic Glucose Sensor Based on Ultrasonic-Electrodeposition of Bimetallic PtM (M=Ru, Pd and Au) Nanoparticles on Carbon Nanotubes−Ionic Liquid Composite Film. *Biosens. Bioelectron.* **2009**, *24*, 3481−3486.

(10) Li, Z.; Xin, Y.; Zhang, Z.; Wu, H.; Wang, P. Rational Design of Binder-Free Noble Metal/Metal Oxide Arrays with Nanocauliflower Structure for Wide Linear Range Nonenzymatic Glucose Detection. *Sci. Rep.* **2015**, *5*, 10617.

(11) Liu, M.; Wang, Y.; Lu, D. Sensitive and Selective Non-Enzymatic Glucose Detection Using Electrospun Porous CuO−CdO Composite Nanofibers. *J. Mater. Sci.* **2019**, *54*, 3354−3367.

(12) Baghayeri, M.; Amiri, A.; Alizadeh, Z.; Veisi, H.; Hasheminejad, E. Non-Enzymatic Voltammetric Glucose Sensor Made of Ternary NiO/Fe3O4-SH/Para-Amino Hippuric Acid Nanocomposite. *J. Electroanal. Chem.* **2018**, *810*, 69−77.

(13) Rahman, M. M.; Ahammad, A. J. S.; Jin, J.-H.; Ahn, S. J.; Lee, J.-J. A Comprehensive Review of Glucose Biosensors Based on Nanostructured Metal-Oxides. *Sensors* **2010**, *10*, 4855−4886.

(14) Yu, R.; Pan, C.; Chen, J.; Zhu, G.; Wang, Z. L. Enhanced Performance of a ZnO Nanowire-Based Self-Powered Glucose Sensor by Piezotronic Effect. *Adv. Funct. Mater.* **2013**, *23*, 5868−5874.

(15) Khatib, K. M. E.; Hameed, R. M. A. Development of CuO_2/Carbon Vulcan XC-72 as Non-Enzymatic Sensor for Glucose Determination. *Biosens. Bioelectron.* **2011**, *26*, 3542−3548.

(16) Wu, J.; Yin, F. Easy Fabrication of a Sensitive Non-Enzymatic Glucose Sensor Based on Electrospinning CuO-ZnO Nanocomposites. *Integr. Ferroelectr.* **2013**, *147*, 47−58.

(17) Li, L.; Du, Z.; Liu, S.; Hao, Q.; Wang, Y.; Li, Q.; Wang, T. A Novel Nonenzymatic Hydrogen Peroxide Sensor Based on MnO_2/Graphene Oxide Nanocomposite. *Talanta* **2010**, *82*, 1637−1641.

(18) Li, X.; Yao, J.; Liu, F.; He, H.; Zhou, M.; Mao, N.; Xiao, P.; Zhang, Y. Nickel/Copper Nanoparticles Modified TiO2 Nanotubes for Non-Enzymatic Glucose Biosensors. *Sens. Actuators, B* **2013**, *181*, 501−508.

(19) Lu, H.; Yu, S.; Fan, Y.; Yang, C.; Xu, D. Nonenzymatic Hydrogen Peroxide Electrochemical Sensor Based on Carbon-Coated SnO2 Supported Pt Nanoparticles. *Colloids Surf., B* **2013**, *101*, 106−110.

(20) Hoa, L. T.; Chung, J. S.; Hur, S. H. A Highly Sensitive Enzyme-Free Glucose Sensor Based on Co3O4 Nanoflowers and 3D Graphene Oxide Hydrogel Fabricated via Hydrothermal Synthesis. *Sens. Actuators, B* **2016**, *223*, 76−82.

(21) Zhang, W.-D.; Chen, J.; Jiang, L.-C.; Yu, Y.-X.; Zhang, J.-Q. A Highly Sensitive Nonenzymatic Glucose Sensor Based on NiO-Modified Multi-Walled Carbon Nanotubes. *Microchim. Acta* **2010**, *168*, 259−265.

(22) Reitz, E.; Jia, W.; Gentile, M.; Wang, Y.; Lei, Y. CuO Nanospheres Based Nonenzymatic Glucose Sensor. *Electroanalysis* **2008**, *20*, 2482−2486.

(23) Wang, X.; Hu, C.; Liu, H.; Du, G.; He, X.; Xi, Y. Synthesis of CuO Nanostructures and Their Application for Nonenzymatic Glucose Sensing. *Sens. Actuators, B* **2010**, *144*, 220−225.

(24) Cao, F.; Gong, J. Nonenzymatic Glucose Sensor Based on CuO Microfibers Composed of CuO Nanoparticles. *Anal. Chim. Acta* **2012**, *723*, 39−44.

(25) Farid, M. M.; Goudini, L.; Piri, F.; Zamani, A.; Saadati, F. Molecular Imprinting Method for Fabricating Novel Glucose Sensor:

Polyvinyl Acetate Electrode Reinforced by MnO_2/CuO Loaded on Graphene Oxide Nanoparticles. *Food Chem.* **2016**, *194*, 61−67.
(26) Luo, L.; Li, F.; Zhu, L.; Zhang, Z.; Ding, Y.; Deng, D. Non-Enzymatic Hydrogen Peroxide Sensor Based on MnO2-Ordered Mesoporous Carbon Composite Modified Electrode. *Electrochim. Acta* **2012**, *77*, 179−183.
(27) Zhang, P.; Zhang, L.; Zhao, G.; Feng, F. A Highly Sensitive Nonenzymatic Glucose Sensor Based on CuO Nanowires. *Microchim. Acta* **2012**, *176*, 411−417.
(28) Wang, J.; Thomas, D. F.; Chen, A. Nonenzymatic Electrochemical Glucose Sensor Based on Nanoporous PtPb Networks. *Anal. Chem.* **2008**, *80*, 997−1004.
(29) Safavi, A.; Maleki, N.; Farjami, E. Fabrication of a Glucose Sensor Based on a Novel Nanocomposite Electrode. *Biosens. Bioelectron.* **2009**, *24*, 1655−1660.
(30) Yin, H.; Zhan, T.; Qin, D.; He, X.; Nie, Q.; Gong, J. Self-Assembly of Dandelion-like NiCo2O4 Hierarchical Microspheres for Non-Enzymatic Glucose Sensor. *Inorg. Nano-Met. Chem.* **2017**, *47*, 1560−1567.
(31) Chandrasekaran, N. I.; Kumari, M.; Muthukumar, H.; Matheswaran, M. Strategy for Multifunctional Hollow Shelled Triple Oxide Mn−Cu−Al Nanocomposite Synthesis via Microwave-Assisted Technique. *ACS Sustain. Chem. Eng.* **2018**, *6*, 1009−1021.
(32) Shao, M.; Ning, F.; Zhao, Y.; Zhao, J.; Wei, M.; Evans, D. G.; Duan, X. Core-Shell Layered Double Hydroxide Microspheres with Tunable Interior Architecture for Supercapacitors. *Chem. Mater.* **2012**, *24*, 1192−1197.
(33) Santos, A.; Kumeria, T.; Losic, D. Nanoporous Anodic Aluminum Oxide for Chemical Sensing and Biosensors. *Trac. Trends Anal. Chem.* **2013**, *44*, 25−38.
(34) Balasubramanian, P.; Annalakshmi, M.; Chen, S.-M.; Chen, T.-W. Ultrasensitive Non-Enzymatic Electrochemical Sensing of Glucose in Noninvasive Samples Using Interconnected Nanosheets-like NiMnO3 as a Promising Electrocatalyst. *Sens. Actuators, B* **2019**, *299*, 126974.
(35) Sinha, L.; Pakhira, S.; Bhojane, P.; Mali, S.; Hong, C. K.; Shirage, P. M. Hybridization of Co3O4 and α-MnO2 Nanostructures for High-Performance Nonenzymatic Glucose Sensing. *ACS Sustain. Chem. Eng.* **2018**, *6*, 13248−13261.
(36) Wang, W.; Zhang, L.; Tong, S.; Li, X.; Song, W. Three-Dimensional Network Films of Electrospun Copper Oxide Nanofibers for Glucose Determination. *Biosens. Bioelectron.* **2009**, *25*, 708−714.
(37) Zhou, C.; Xu, L.; Song, J.; Xing, R.; Xu, S.; Liu, D.; Song, H. Ultrasensitive Non-Enzymatic Glucose Sensor Based on Three-Dimensional Network of ZnO-CuO Hierarchical Nanocomposites by Electrospinning. *Sci. Rep.* **2014**, *4*, 7382.
(38) Weina, X.; Guanlin, L.; Chuanshen, W.; Hu, C.; Wang, X. A Novel β-MnO_2 Micro/Nanorod Arrays Directly Grown on Flexible Carbon Fiber Fabric for High-Performance Enzymeless Glucose Sensing. *Electrochim. Acta* **2017**, *225*, 121−128.
(39) Jiang, L.-C.; Zhang, W.-D. A Highly Sensitive Nonenzymatic Glucose Sensor Based on CuO Nanoparticles-Modified Carbon Nanotube Electrode. *Biosens. Bioelectron.* **2010**, *25*, 1402−1407.
(40) Wang, Y.; Bai, W.; Nie, F.; Zheng, J. A Non-Enzymatic Glucose Sensor Based on Ni/MnO_2 Nanocomposite Modified Glassy Carbon Electrode. *Electroanalysis* **2015**, *27*, 2399−2405.
(41) Zhang, J.; Ma, J.; Zhang, S.; Wang, W.; Chen, Z. A Highly Sensitive Nonenzymatic Glucose Sensor Based on CuO Nanoparticles Decorated Carbon Spheres. *Sens. Actuators, B* **2015**, *211*, 385−391.
(42) Ahmad, R.; Tripathy, N.; Hahn, Y.-B.; Umar, A.; Ibrahim, A. A.; Kim, S. H. A Robust Enzymeless Glucose Sensor Based on CuO Nanoseed Modified Electrodes. *Dalton Trans.* **2015**, *44*, 12488−12492.
(43) Guo, C.; Li, H.; Zhang, X.; Huo, H.; Xu, C. 3D Porous CNT/MnO2 Composite Electrode for High-Performance Enzymeless Glucose Detection and Supercapacitor Application. *Sens. Actuators, B* **2015**, *206*, 407−414.
(44) Muthuchamy, N.; Atchudan, R.; Edison, T. N. J. I.; Perumal, S.; Lee, Y. R. High-Performance Glucose Biosensor Based on Green Synthesized Zinc Oxide Nanoparticle Embedded Nitrogen-Doped Carbon Sheet. *J. Electroanal. Chem.* **2018**, *816*, 195−204.

https://dx.doi.org/10.1021/acsomega.0c00417
ACS Omega 2020, 5, 23502−23509